Time of flight and direction of arrival of HF radio signals received over a path along the midlatitude trough: Observations

D. R. Siddle, A. J. Stocker, and E. M. Warrington

Department of Engineering, University of Leicester, Leicester, UK

Received 18 February 2004; revised 31 May 2004; accepted 11 June 2004; published 17 August 2004.

[1] Measurements of the time-of-flight, direction of arrival, and Doppler spread are presented for HF radio signals radiated on six frequencies between 4.6 and 18.4 MHz received over a subauroral path oriented along the midlatitude trough between Sweden and the UK. During the day, the signals usually arrived from the great circle direction whereas at night, especially during the winter and equinoctial months; the signals on frequencies between 7.0 and 11.1 MHz often arrived from directions well displaced from the great circle direction. In summer the deviations tended to be smaller (<5°) than those observed during the other seasons (several tens of degrees). The deviations were mainly to the north and often lasted all night, with the time of flight initially decreasing and then increasing, showing an approach and then recession of the reflection point. Southerly deviations were much less coherent and less frequent. *INDEX TERMS:* 2439 Ionosphere: Ionospheric irregularities; 6934 Radio Science: Ionospheric propagation (2487); 6964 Radio Science: Radio wave propagation; *KEYWORDS:* midlatitude trough, ionospheric HF propagation

Citation: Siddle, D. R., A. J. Stocker, and E. M. Warrington (2004), Time of flight and direction of arrival of HF radio signals received over a path along the midlatitude trough: Observations, *Radio Sci.*, *39*, RS4008, doi:10.1029/2004RS003049.

1. Introduction

[2] The midlatitude trough is an area of depleted electron density in the nighttime *F* region ionosphere in which the critical frequencies drop by a factor of at least two and the altitude of the electron density peak rises by 100 km or more [*Moffett and Quegan*, 1983]. During the winter and equinoctial months, the trough takes the form of a band a few degrees wide in latitude to the equatorward side of the auroral oval, stretching in local time from dusk to dawn. In summer, the trough is much less pronounced and is confined to the hours around midnight. The location of the trough also depends on geomagnetic activity; the trough region moving equatorward and the evening sector tending to move to earlier local times as activity increases.

[3] The presence of the trough has a significant impact on a number of radio systems. For transionospheric signals, the reduction in total electron content over the trough region affects the time of flight of the signals which, for example, may lead to incorrect ionospheric corrections and hence timing and positional errors in satellite based navigation systems such as GPS and the forthcoming European Galileo system. For HF systems, the principle concern of this paper, the electron density depletion in the trough region reduces the maximum frequency that can be reflected by the ionosphere along the great circle path (GCP). Gradients in electron density associated with the trough walls and embedded ionospheric irregularities often result in propagation in which the signal path is well displaced from the great circle direction, with directions of arrival at the receiver offset by up to 100° [*Rogers et al.*, 1997]. For long paths, the electron density depletion suppresses propagation along the great circle, and the signal is often received via a ground/sea-scatter mechanism to the side of the great circle direction [*Stocker et al.*, 2003]. Deviations from the great circle direction impact not only on radiolocation systems for which estimates of a transmitter location are obtained by triangulation from a number of receiving sites, but also on any radio communications system in which directional antennas are employed. Furthermore, the Doppler and multimode delay spread characteristics of the signal are also affected when propagation is via scatter/reflection from irregularities in or close to the north wall of the trough [*Warrington et al.*, 1997; *Warrington and Stocker*, 2003]. Rapid deterioration in achievable data throughput in digital communications links occurs when the delay and Doppler spreads exceed system-dependent values [*Angling et al.*, 1998], and hence it is desirable that full account be taken of these

0048-6604/04/2004RS003049$11.00

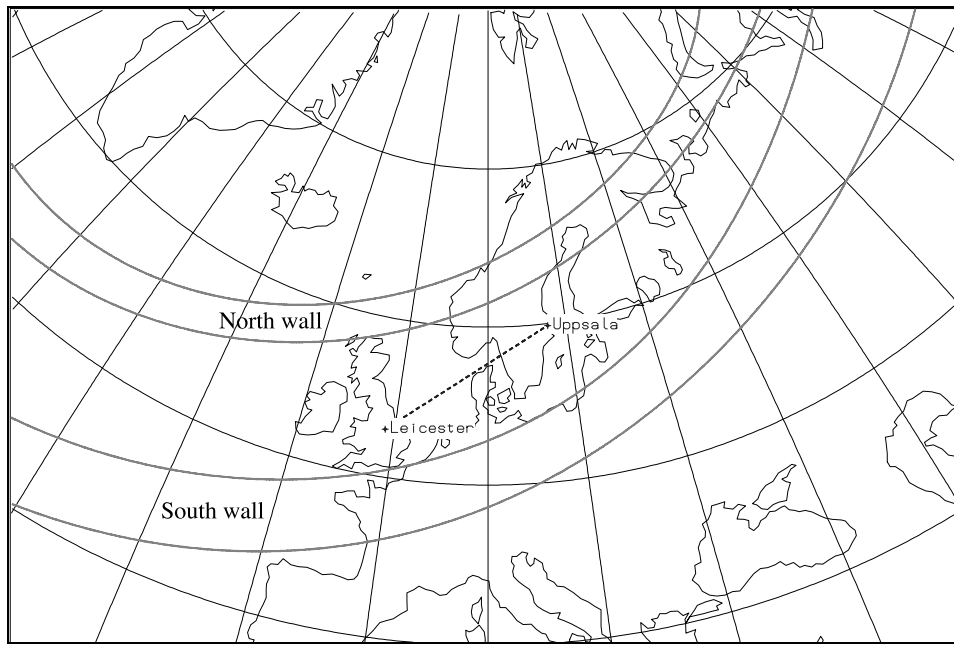

Figure 1. A map showing propagation between Uppsala and Leicester and a typical position for the trough, as estimated by the model of *Halcrow and Nisbet* [1977] for 0000 UT on 11 March 2001. The four lines indicate the outer and inner edges of the north and south walls.

propagation mechanisms in planning and operating HF communication systems.

[4] The trough has been modeled on a statistical basis by various researchers [see, e.g., *Halcrow and Nisbet*, 1977; *Hanbaba*, 1999; *Rothkaehl et al.*, 2000; *Feichter and Leitinger*, 2001]. Recent developments in ionospheric tomography [*Kersley et al.*, 1997; *Mitchell et al.*, 1997] and observations made with EISCAT [*Jones et al.*, 1997] have provided further experimental observations of the trough position and structure. In this paper, measurements are presented of the direction of arrival (DOA) and the time of flight (TOF) of HF signals received over a 1400 km path oriented along the trough between Uppsala, Sweden and the University of Leicester's field site near to Leicester (see Figure 1). The experiment was operational between October 2000 and January 2002.

2. Observations

[5] Six frequencies were used during the experiment, namely 4.6, 7.0, 10.4, 11.1, 14.4, and 18.4 MHz. Transmissions on each frequency were made over a period of thirty seconds with an overall cycle time of 3 min. Each transmission period contained two 13-bit Barker-coded BPSK transmissions each of 2 s duration with a chip rate of 1667 baud. Both the transmitter and the receiver system clocks were synchronized to GPS so that the direction of arrival and signal strength could be measured as a function of absolute time of flight. The direction of arrival of the various signal components was estimated using the Capon superresolution algorithm [*Capon*, 1969; *Featherstone et al.*, 1997]. As an additional diagnostic, a BR Communications chirpsounder system was deployed with the transmitter collocated with the main transmitter in Uppsala and the receiver at the University of Leicester.

2.1. Example Measurements

[6] Measurements at 10.4 MHz are presented in Figure 2. These are typical of those found throughout the entire data set for the 7.0 to 11.1 MHz signals. The large deviations occur less frequently at the other frequencies. During the day, the signal strength versus time of flight plot (top left panel) indicates the presence of 3 modes, identified as 1F, 2F and 3F. The azimuthal angle of arrival (second left panel) is close to the GCP (46°) for each mode while the elevation angle (third left panel) is around 10°, 20° and 40° respectively. The frequency spectrum (bottom left panel) shows a narrow peak. The method employed by *Angling et al.* [1998] is adopted here to quantify Doppler spread in which

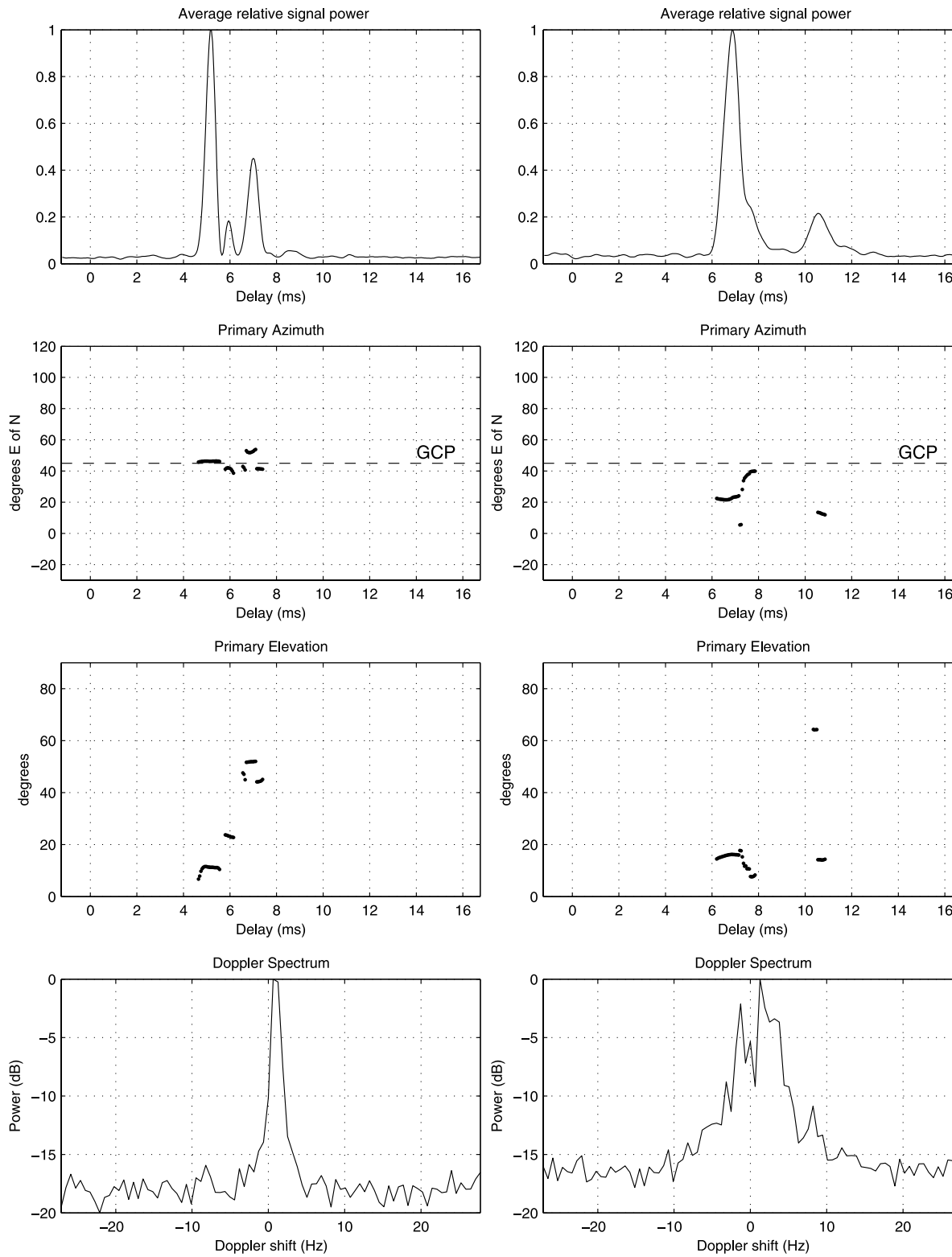
Average relative signal power
Delay (ms)
Primary Azimuth
degrees E of N
GCP
Primary Elevation
degrees
Doppler Spectrum
Power (dB)
Doppler shift (Hz)

Figure 2

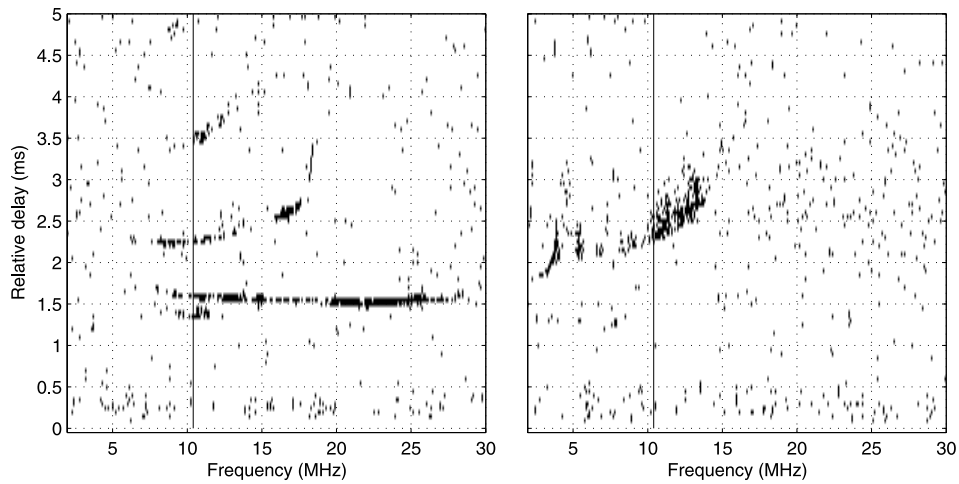

Figure 3. Oblique ionograms for (left) 1136 UT and (right) 0206 UT on 23 November 2001 (day 327). The vertical line indicates 10.4 MHz.

composite Doppler spread is defined as the narrowest spectral width which contains 80% of the power. In these terms, the spread in the daytime example of Figure 2 is 1.3 Hz. At night (right hand panels in Figure 2) two modes are evident: a narrow one at a TOF of just less than 7 ms (i.e., at about the same delay as the 3F daytime mode) and a second, slightly broader, mode with a longer TOF. The azimuthal direction of both modes is about 25° to the north of the GCP (note there appears to be a small variation in the bearing within each mode, e.g., the tail edge of the first mode is only about 5° north of the GCP) and elevation angles in the range 10°–17°. A somewhat broader frequency spectrum is observed than that for the daytime case, with a composite Doppler spread of 5 Hz.

[7] Figure 3 shows oblique ionograms taken along the Uppsala-Leicester path for nighttime and daytime on the same day. The ionogram on the left was recorded at 1134 UT, and shows the three *F* region modes seen in Figure 2 with an MUF around 28 MHz and an E mode below the 1F trace. The ionogram on the right was taken at 0206 UT and displays the expected nighttime 1F trace which has a maximum frequency of about 4 MHz and a 'spread' echo extending up to about 14 MHz. Note that the ionograms recorded around midnight exhibit similar features however the contrast is low making them less suitable for reproduction here. For a discussion of ionogram features observed over paths along the trough, see *Rogers et al.* [2003].

[8] The TOF, bearing, elevation, Doppler shift and spread and carrier to noise ratio measurements made over three days in November 2001 at 10.4 MHz are shown in Figure 4. As for the data presented in Figure 2, the daytime signals frequently exhibit 1-hop, 2-hop and 3-hop *F* region propagation along the GCP (see TOF plots). The Doppler spread is low and the signal is relatively strong, reduced only by *D* region absorption in the middle of the day. At night, a wider variety of effects are observed. On the first night (day 324–325), the daytime trace deviates northward at sunset and is then replaced by intermittent *E* region propagation on the GCP. The signal strength is about 20 dB lower than the daytime value and Doppler spread is low. On the second night (day 325–326), just after midnight, propagation occurs via a mode with a relatively long TOF (8–10 ms) and direction of arrival 40°–60° to the north of the GCP. The signal is around 20 dB weaker than the daytime values with a Doppler shift of up to about 5 Hz. The most striking behavior can be observed on the third night (day 326–327) where a propagation mode appears at a long TOF (up to 13 ms) at about 2030 UT. Over the next

Figure 2. Example measurements made at 10.4 MHz of signals received near Leicester on 23 November 2001 (day 327) for daytime (1134 UT, left) and nighttime (0004 UT, right). From the top, the panels represent signal strength (linear, normalized) versus time-of-flight (ms), azimuth (degrees) versus time-of-flight (ms), elevation (degrees) versus time-of-flight (ms), and amplitude (dB) versus Doppler frequency (Hz). The three daytime and two nighttime modes in the upper panels sometimes appear to be subdivided by direction of arrival. Care must be taken in interpreting these measurements when the signal amplitude is low (e.g., toward the leading and trailing edges of the received pulses).

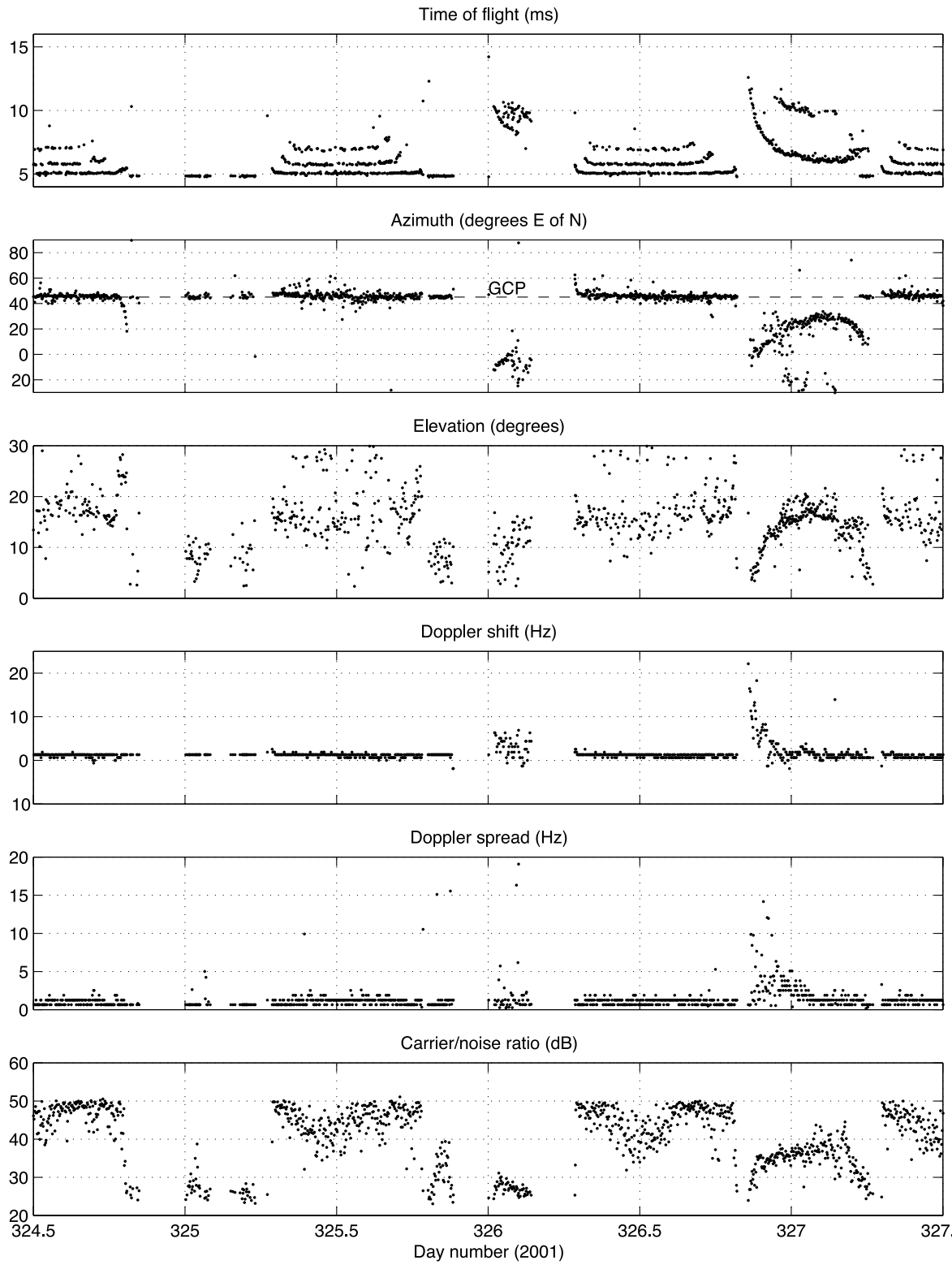
Time of flight (ms)
15
10
5
Azimuth (degrees E of N)
80
60
40
20
0
20
GCP
Elevation (degrees)
30
20
10
0
Doppler shift (Hz)
20
10
0
10
Doppler spread (Hz)
20
15
10
5
0
Carrier/noise ratio (dB)
60
50
40
30
20
324.5
325
325.5
326
326.5
327
327.5
Day number (2001)

Figure 4

Table 1. Occurrence Statistics by Mode and Bearing for Signal Frequencies of 7.0, 10.4, 11.1, and 14.4 MHz[a]

	VOACAP	Observations				
	No Propagation	No Propagation	Long Time of Flight	GCP	Northerly Deviations	Southerly Deviations
			7.0 MHz			
Spring	11	8	31	82	41	2
Summer	1	0	4	99	11	4
Autumn	13	0	17	95	38	4
Winter	65	8	64	47	80	1
			10.4 MHz			
Spring	61	35	42	41	48	0
Summer	23	2	21	91	37	2
Autumn	82	13	60	55	69	0
Winter	99	36	57	3	57	0
			11.1 MHz			
Spring	71	61	35	18	31	0
Summer	33	3	29	93	39	2
Autumn	77	34	58	23	57	0
Winter	100	44	55	1	47	0
			14.4 MHz			
Spring	97	96	4	0	4	0
Summer	88	65	7	37	8	0
Autumn	99	82	16	0	13	0
Winter	100	76	18	0	14	0

[a]All figures represent percentages with respect to the number of nights for which measurements were made during 2001 (297 nights). Since several directions of arrival (on-GCP, northerly and/or southerly) are possible on any given night, the percentages may total more than 100%.

six hours, the TOF decreases reaching a steady value of about 7 ms by 0230 UT. At times around midnight a weaker, second mode at a longer delay (~11 ms) is present (cf. Figure 2). As the TOF decreases, the bearing deviation from great circle decreases from about 40° north at 2030 UT to 20° north at 0230 UT, the elevation angle increases from around 10° to 15–20° and the signal strength attains a level only about 10 dB below the daytime, on-GCP level. The rapid decrease in TOF is accompanied by a strong positive Doppler shift (~20 Hz). The Doppler spread is higher than daytime values until the direction of arrival deviates northward (around 0300 UT) when it is about the same as during the day.

2.2. Occurrence Statistics

[9] Table 1 shows the percentage of nights on which various features are seen for the four central frequencies in the experiment. The seasons are defined according to ITU recommendation P1148 [*International Telecommunication Union* (*ITU*), 1997], with spring including all of March and April, summer including May to August, autumn September and October and winter November to February. In deriving these statistics, propagation is deemed to have occurred if any readily identifiable trace, other than sporadic E, is seen between 2100 and 0300 UT. However, during some intervals, the data quality was not sufficient to categorize the direction of arrival and these together with the short-lived deviations that sometimes occur briefly at dawn and dusk (see, e.g., sunrise on day 326 in Figure 4) have been excluded. The nighttime feature observed on day 326–327 (a long TOF accompanied by northerly bearing deviations of up to 50° and Doppler shifts) is a relatively common occurrence in the nonsummer months. During the summer, the deviation in azimuth tended to be much smaller (<5°) but still generally to the north. Deviations to the south are very rare, small in angle and short-lived. Table 1 also shows the percentage of nights when no propagation is

Figure 4. Measurements made at 10.4 MHz between noon on 20 November 2001 (day 324) and noon on 23 November 2001 (day 327). From top to bottom, the panels represent time-of-flight (ms), azimuth of strongest mode (degrees), elevation of strongest mode (degrees), Doppler shift (Hz), Doppler spread (Hz), and carrier to noise ratio (dB).

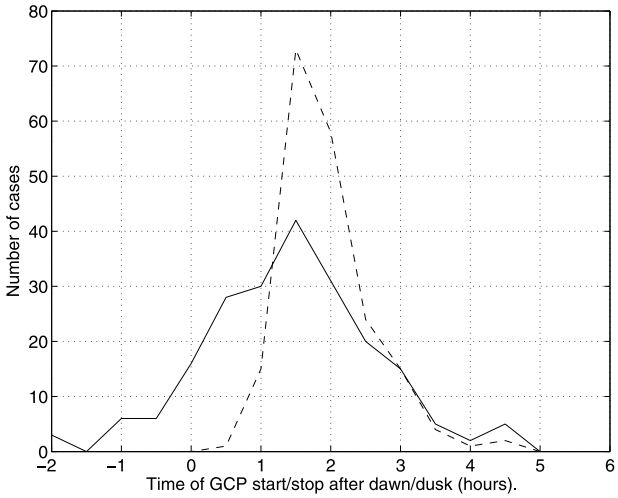

Figure 5. Plot of the time after sunset at which the 1F main daytime mode of GCP propagation ceases (solid) and of time after sunrise at which it starts again (dashed) for 10.4 MHz. Sunset and sunrise were calculated at a point 300 km above Earth's surface at the midpoint of the GCP on the basis of 200 data points for the cessation of on-GCP propagation and 193 data points for the start of on-GCP propagation. Days 1–123 and 235–365 of 2001.

predicted by VOACAP. VOACAP computes monthly medians of propagation likelihood for a given hour of the day, and the hour in the period 2100–0300 UT with the highest probability of propagation is taken to be representative of the probability of propagation for that night. The probability is averaged over the relevant months to give the value presented in Table 1. Sporadic E propagation is excluded, as the model used in VOACAP to predict this can give misleading results [*Lane*, 2001]. While VOACAP does not explicitly include a model of the trough, its effect may be present to some extent in the underlying CCIR maps of the various ionospheric propagation parameters, e.g., M(3000). For all frequencies, VOACAP underestimates how often propagation occurs. The frequencies shown in Table 1 define the limits of the off-GCP propagation for this path. For the remaining frequencies: at 4.6 MHz, GCP propagation is seen almost every night, and no clear long TOF events can be distinguished, whereas at 18.4 MHz, propagation is only seen at night two or three times in the whole study.

[10] The azimuthal deviations may be compared to those seen by Rogers, *Warrington et al.* [1997] over paths which traversed the midlatitude trough. Using frequencies 5.1, 10.9 and 15.9 MHz, they observed deviations to the north and south of approximately equal size and frequency. The deviations had similar seasonal and diurnal variations as seen here, and were accompanied by Doppler spread. The differences between these two experiments are explored in further detail in the article which accompanies this [*Siddle et al.*, 2004].

[11] The solid curve of Figure 5 indicates the time after sunset at which the 1F main daytime mode of GCP propagation ceases, while the dashed line indicates the time after sunrise at which GCP recommences. Sunset and sunrise were calculated at a point 300 km above Earth's surface at the mid point of the GCP. Variation of this position laterally by ±3° or vertically by ±200 km made only about 10% difference to the standard deviation of the distributions, but caused a shift in the distributions with respect to dusk or dawn by about an hour. Data from May to August of 2001, when the Sun does not set at this altitude and location, are excluded from this analysis. Even during the included times, GCP propagation is sometimes detected between the end of the main mode and its start on the following day, either via *E* or *F* region propagation. Nevertheless, there is usually a cusp as the TOF increases sharply close to sunrise and sunset, and this is taken to be the beginning or end of the main daytime mode. It can be seen that the start of the main daytime mode is more highly correlated to sunrise than the end is to sunset. This is expected from the different processes governing production and decay of ionization and the occurrence time of the trough which depends on the level of geomagnetic activity.

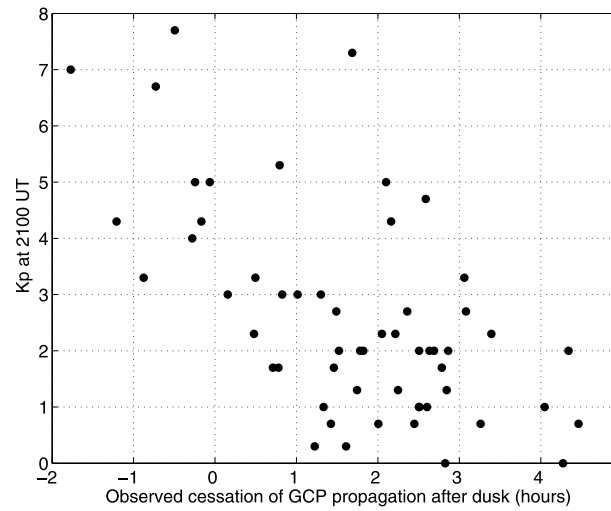

Figure 6. Time of cessation of 10.4 MHz GCP propagation after dusk at GCP midpoint and 300 km altitude versus Kp for September and October of 2001. (Note that Kp readings of n− and n+ are evaluated as n − 0.3 and n + 0.3, respectively).

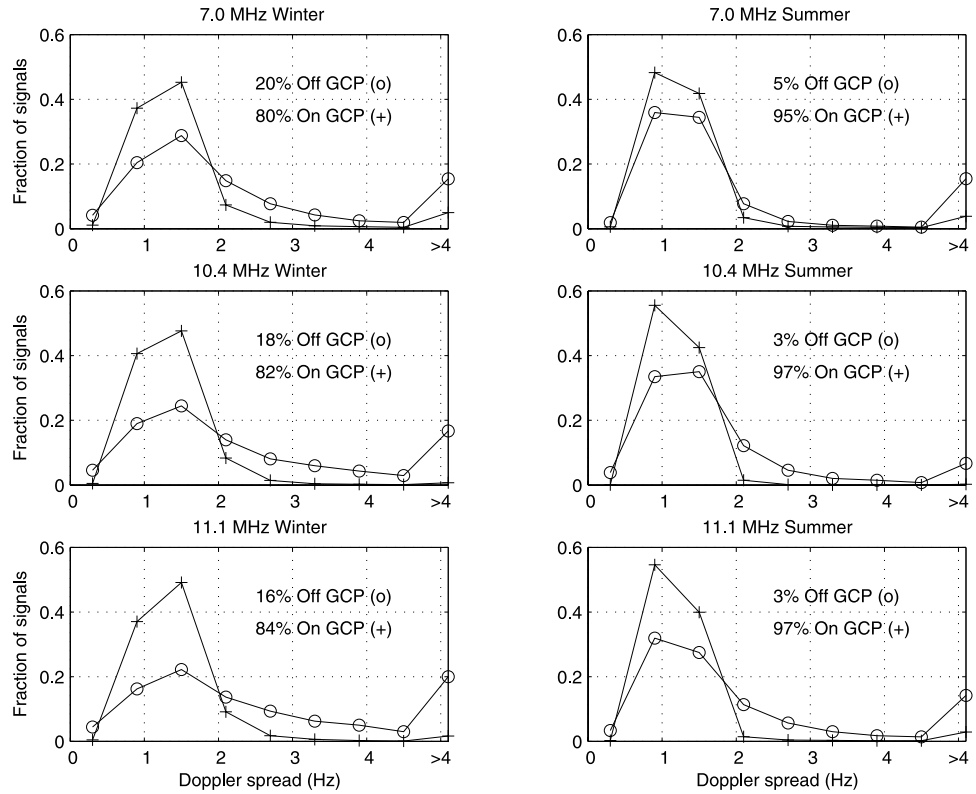

Figure 7. Plots of Doppler spread for all data taken in 2001. From top to bottom: frequencies 7.0, 10.4, and 11.1 MHz. Data are divided by azimuth of arrival: crosses for GCP, circles for off-GCP. The area under each curve is the same, and relative contributions to the whole are indicated as percentages. Note that the resolution of the Doppler data is approximately 0.6 Hz, so a point at 0.3 Hz represents all data in the first FFT bin (0–0.6 Hz) and at 0.9 Hz represents all data in the second FFT bin (0.6–1.2 Hz), etc.

Figure 6 shows the delay between sunset and the end of GCP propagation at 10.4 MHz plotted against the Kp observed at 2100 UT, for autumn nights. A correlation coefficient of around −0.60 was obtained showing that low magnetic activity allows GCP propagation to continue later into the evening. A similar plot for spring gives a correlation of −0.56, but a much lower correlation of −0.25 is obtained for winter. The difference between winter and equinox in 2001 may in part be due to the quiet geomagnetic conditions observed in the winter months (Kp does not exceed 5). Together, Figures 5 and 6 show that the solar zenith angle and level of geomagnetic activity (indicated by Kp) are controlling factors as to whether or not propagation along the great circle path is supported, and corroborating evidence that the off-GCP propagation is due to the presence of the trough.

[12] Figure 7 shows the spread seen in the Doppler measurements for the 7.0, 10.4 and 11.1 MHz signals occurring throughout the day. It includes all data whose azimuth of arrival lies between 0° (north) and 90° (east). Azimuth is divided into on-GCP, between 35° and 55°, and off-GC outside this range. The relative scarcity and indefiniteness of southerly signals precludes separate treatment of northerly and southerly signals here. All the distributions shown in Figure 7 have a lower decile at 0.6 Hz (equal to the resolution of the Doppler spread), but the upper deciles exhibit differences. For GCP signals, all frequencies give an upper decile of 1.9 Hz in the winter and 1.3 Hz in the summer. Off-GCP signals are more spread, with upper deciles of 8.2, 7.6 and 9.2 Hz for 7.0, 10.4 and 11.1 MHz respectively in winter and 14.1, 3.2 and 8.8 Hz for 7.0, 10.4 and 11.1 MHz respectively in summer. For comparison, the particular off-GCP event on day 326–327 in Figure 4 lies within the 0°–35°azimuth band and has an upper decile of 4.4 Hz. The fact that the (mostly northerly) off-GCP signals have generally higher values of Doppler spread is

consistent with scattering from irregularities in the north wall and/or auroral oval.

3. Conclusions

[13] The establishment of a multifrequency HF circuit between Uppsala and Leicester has allowed us to observe simultaneously the direction of arrival, time of flight, Doppler shift and Doppler spread of signals reflected from the ionosphere. During the day, the measurements usually show propagation via the *F* region along the GCP with little Doppler spread. At night, however, off-great circle propagation often occurs which may be via reflection from the north wall of the midlatitude trough or by scatter from irregularities embedded within the wall or slightly to the north when the oval and trough wall do not coincide. This type of off-GCP propagation occurs on nights when none is predicted by VOACAP and preferentially in winter and near equinox. The strongest examples of off-GCP reflection are seen at frequencies 7.0, 10.4 and 11.1 MHz. Southerly deviations are much less frequent and smaller in angle and duration.

[14] Measurements indicate that signals arriving at night from north of the GCP often have a greater Doppler spread than those arriving on-GCP. Spread traces are also seen on the oblique ionograms taken at time of northerly reflection, indicating that the propagation mechanism differs from that for GCP. The latter are consistent with reflection from electron density gradients, while the former suggests scattering from irregularities.

[15] That the off-GCP propagation is controlled by the midlatitude trough is shown by its dependence on solar radiation at the point of reflection. This dependence is more direct for sunrise, whereas the start of propagation at sunset depends also on Kp.

[16] The mechanisms by which off-great circle path propagation occurs have been investigated through simulation, the results of which are reported by in the companion paper by *Siddle et al.* [2004].

[17] **Acknowledgments.** The authors would like to thank the Swedish Meteorological Institute for hosting the transmitter at their Marsta site. This investigation was supported by a grant from the EPSRC.

References

Angling, M. J., P. S. Cannon, N. C. Davies, T. J. Willink, V. Jodalen, and B. Lundborg (1998), Measurements of Doppler and multipath spread on oblique high latitude HF paths and their use in characterising data modem performance, *Radio Sci.*, *33*(1), 97–107.

Capon, J. (1969), High resolution frequency-wavenumber spectrum analysis, *IEEE Proc.*, *57*, 1408–1419.

Featherstone, W., H. J. Strangeways, M. A. Zatman, and H. Mewes (1997), A novel method to improve the perform ance of Capon's minimum variance estimator, in *Proceedings of the IEE 10th International Conference on Antennas and Propagation*, pp. 1.322–1.325, Inst. of Electr. Eng., London.

Feichter, E., and R. Leitinger (2001), Properties of the main trough of the F region derived from Dynamic Explorer 2 data, *Annal. Geophys.*, *45*(1), 117–124.

Halcrow, B. W., and J. S. Nisbet (1977), A model of the F2 peak electron densities in the main trough region of the ionosphere, *Radio Sci.*, *12*, 815–820.

Hanbaba, B. (1999), COST 251: Improved quality of service in ionospheric telecommunication systems planning and operation: Final report, Space Res. Cent., Warsaw, Poland.

International Telecommunication Union (ITU) (1997), Standardized procedure for comparing predicted and observed HF sky-wave signal intensities and the presentation of such comparisons, ITU-R Recomm. P1148–1, paragraph 3.5, Geneva.

Jones, D. G., I. K. Walker, and L. Kersley (1997), Structure of the poleward wall of the trough and the inclination of the geomagnetic field above the EISCAT radar, *Annal. Geophys.*, *15*, 740–746.

Kersley, L., S. E. Pryse, I. K. Walker, J. A. T. Heaton, C. N. Mitchell, M. J. Williams, and C. A. Willson (1997), Imaging of electron density troughs by tomographic techniques, *Radio Sci.*, *32*, 1607–1621.

Lane, G. (2001), *Signal-to-Noise Predictions Using VOACAP, Including VOAARSA*, Rockwell-Collins, Iowa.

Mitchell, C. N., L. Kersley, and S. E. Pryse (1997), The effects of receiver location in two-station experimental ionospheric tomography, *J. Atmos. Sol. Terr. Phys.*, *59*, 1411–1415.

Moffett, R. J., and S. Quegan (1983), The mid-latitude trough in electron concentration of the ionospheric F-layer: A review of observations and modelling, *J. Atmos. Sol. Terr. Phys.*, *45*, 315–343.

Rogers, N. C., E. M. Warrington, and T. B. Jones (1997), Large HF bearing errors for propagation-paths tangential to the auroral oval, *IEE Proc. Microwaves Antennas Propaga.*, *144*(2), 91–96.

Rogers, N. C., E. M. Warrington, and T. B. Jones (2003), Oblique ionogram features associated with off-great-circle HF propagation at high and sub-auroral latitudes, *IEE Proc. Microwaves Antennas Propagat.*, *150*(4), 295–300, doi:10.1049/ip-map:20030552.

Rothkaehl, H., I. Stanislawska, R. Leitinger, and Y. Tulunay (2000), Application of a trough model for telecommunication purposes, *Phys. Chem. Earth, Part C*, *25*, 315–318.

Siddle, D. R., N. Y. Zaalov, A. J. Stocker, and E. M. Warrington (2004), Time of flight and direction of arrival of HF radio signals received over a path along the mid-latitude trough: Theoretical considerations, *Radio Sci.*, *39*, RS4009, doi:10.1029/2004RS003052.

Stocker, A. J., E. M. Warrington, and T. B. Jones (2003), A comparison of observed and modelled deviations from the great circle direction for a 4490 km HF propagation path along the mid-latitude ionospheric trough, *Radio Sci.*, *38*(3), 1054, doi:10.1029/2002RS002781.

Warrington, E. M., and A. J. Stocker (2003), Measurements of the Doppler and multipath spread of HF signals received over a path oriented along the mid-latitude trough, *Radio Sci.*, *38*(5), 1080, doi:10.1029/2002RS002815.

Warrington, E. M., T. B. Jones, and B. S. Dhanda (1997), Observations of the Doppler spread on HF signals propagated over high-latitude paths, *IEE Proc. Microwaves Antennas Propagat.*, *144*(4), 215–220.

D. R. Siddle, A. J. Stocker, and E. M. Warrington, Department of Engineering, University of Leicester, Leicester LE1 7RH, UK. (emw@leicester.ac.uk)